

THE INEVITABLE FUTURE OF THE STARLESS CORE BARNARD 68

ANDREAS BURKERT¹ AND JOÃO ALVES²

Submitted to ApJ

ABSTRACT

Dense, small molecular cloud cores have been identified as the direct progenitors of stars. One of the best studied examples is Barnard 68 which is considered a prototype stable, spherical gas core, confined by a diffuse high-pressure environment. Observations of its radial density structure however indicate that Barnard 68 should be gravitationally unstable and collapsing which appears to be inconsistent with its inferred long lifetime and stability. We argue that Barnard 68 is currently experiencing a fatal collision with another small core which will lead to gravitational collapse. Despite the fact that this system is still in an early phase of interaction, our numerical simulations imply that the future gravitational collapse is already detectable in the outer surface density structure of the globule which mimicks the profile of a gravitationally unstable Bonnor-Ebert sphere. Within the next 2×10^5 years Barnard 68 will condense into a low-mass solar-type star(s), formed in isolation, and surrounded by diffuse, hot interstellar gas. As witnessed in situ for Barnard 68, core mergers might in general play an important role in triggering star formation and shaping the molecular core mass distribution and by that also the stellar initial mass function.

Subject headings: ISM: globules – ISM: clouds – ISM individual (Barnard 68) – stars: formation – hydrodynamics

1. INTRODUCTION

Barnard 68 is considered an excellent test case and the prototype of a dense molecular cloud core (Alves et al. 2001b). Because of its small distance (~ 125 pc), this so called Bok globule (Bok & Reilly 1947) with a mass of $M=2.1 M_{\odot}$, contained within a region of $R = 12,500$ AU has been observed with unprecedented accuracy (Alves et al. 2001b; Lada et al. 2003; Bergin et al. 2006; Redman et al. 2006; Maret et al. 2007). Deep near-infrared dust extinction measurements of starlight toward individual background stars observed through the cloud provided a detailed 2-dimensional map of its projected surface density distribution (Fig. 1) from which a high-resolution density profile was derived over the entire extent of the system. The striking agreement of the inferred density structure with the theoretical solution of an isothermal, pressure confined, hydrostatic gas sphere (so called Bonnor-Ebert sphere) was interpreted as a signature that the globule is old, thermally supported and stable, with the pressure gradient balancing the gravitational force.

This conclusion has received additional support from molecular line observations (Lada et al. 2003) that show complex profile shapes which can be interpreted as signatures of stable oscillations (Redman et al. 2006; Broderick et al. 2007) with subsonic velocities of order $V \approx 0.04$ km/s which is 20% of the isothermal sound speed $c_s \approx 0.2$ km/s. The age of Barnard 68 should therefore be larger than one dynamical oscillation timescale $\tau_{dyn} = 2R/V = 3 \times 10^6$ yrs which is long compared to its gravitational collapse timescale $\tau_{coll} = (3\pi/32G\rho)^{1/2} = 0.17 \times 10^6$ years, where $\rho = 1.5 \times 10^{-19}$ g cm⁻³ is the average mass

density. The observed hydrostatic profile and the inferred large age are strong arguments for stability.

Other observations however are in conflict with this conclusion. The best fitting hydrostatic model leads to the conclusion that Barnard 68 should be gravitationally unstable (Alves et al. 2001b). Pressure confined, self-gravitating gas spheres with radii R and isothermal sound speeds c_s have self-similar density distributions (see Appendix) that are characterized by the dimensionless parameter

$$\xi_{max} = \frac{R}{c_s} \sqrt{4\pi G \rho_c} \quad (1)$$

where ρ_c is the central density. Although all values of $\xi_{max} > 0$ represent equilibrium solutions where the gravitational force is exactly balanced by pressure forces, a stability analyses (Bonnor 1956) shows that small perturbations should lead to gravitational collapse in cores with $\xi_{max} > 6.5$. Barnard 68's surface density distribution is characterised by $\xi_{max} = 6.9 \pm 0.2$. It should collapse on a free-fall timescale which is much shorter than its oscillation timescale. In addition, the question arises how this globule could ever achieve an unstable equilibrium state in the first place.

Dense molecular cores like Barnard 68 are the last well characterized configuration of interstellar gas before gravitational collapse towards star formation. They have masses from a tenth to tenths of solar masses and typical sizes from a tenth to a few tenths of a parsec (Alves et al. 2007). They are found in isolation, known then as Bok globules (Bok 1948), or embedded in lower density molecular cloud complexes. Because of their relatively simple shapes they have long been recognized as important laboratories to the process of star formation. Barnard 68 is one such dense core. Despite being isolated and surrounded by warm and diffuse gas it is part of the Pipe Nebula complex (Alves et al. 2007; Lombardi et al. 2006;

¹ University Observatory Munich, Scheinerstrasse 1, D-81679 Munich

² Calar Alto Observatory, C. Jesús Durbán Remón, 2-2, E-4004 Almeria, Spain

Electronic address: burkert@usm.uni-muenchen.de, jalves@caha.es

Lada et al. 2008) which consists of an ensemble of about 200 cores within a region of order 10 pc. Many cores appear distorted and asymmetric. This could be a result of their interaction with the highly turbulent diffuse gas environment that leads to non-linear and non-radial oscillations (Broderick et al., 2007, 2008). Another possibility which we will investigate here are collisions between cores. We propose that Barnard 68 is currently experiencing such a fatal collision that triggers gravitational collapse. Its peculiar and seemingly contradictory properties are early signatures of this process that cannot be understood if the globule is treated as an isolated and stable Bonnor-Ebert sphere. Observations show that the distribution of molecular core masses is surprisingly similar to the stellar initial mass function (Alves et al. 2007). This indicates that the masses of stars originate directly from the processes that shape the molecular core mass function. Barnard 68 demonstrates that core-core collisions could play an important role in this process.

2. EVIDENCE FOR A COLLISION

The surface density map of Barnard 68 (upper panel of Fig. 1) clearly shows a southeastern prominence which appears to be a separate smaller globule (the bullet) that is currently colliding with its larger companion (the main cloud). From the bullet's surface density distribution we infer a gas mass of $0.2 M_{\odot}$ masses which is 10% the mass of the main cloud. Note that the bullet appears tidally elongated, probably along its orbit that is oriented perpendicular to the line of sight. Such a distortion is expected if the mutual gravitational attraction could affect the bullet during its approach, that is if its encounter velocity is of order or smaller than $(GM/R)^{1/2} \approx 0.4$ km/s.

One might argue that the apparent collision is a projection effect and that B68 and the bullet are two isolated equilibrium clouds. There is however strong evidence for the merger scenario. First of all, the bullet clearly shows substructure (Fig. 1). It consists of two embedded components which indicates that the bullet itself is part of a merger. If the bullet would be isolated, pressure confined and as long-lived as B68 it would not have two density peaks. This indicates that mergers occur in the Pipe nebula. If the two small substructures in the bullet formed by a merger despite their small geometrical cross section, it is even more likely that B68 can capture a clump due to its large cross section and larger gravitational force. In addition, the lower panel of figure 1 shows that B68, the two substructures in the bullet and the other clumps in the vicinity of B68 are not randomly oriented but aligned like pearls on a string. Numerical simulations (e.g. Burkert & Bodenheimer 1993, 1996; Truelove et al. 1998; Burkert & Hartmann 2004) of molecular cloud collapse and star formation demonstrate that such a situation can arise naturally when elongated gas clouds and sheets become gravitationally unstable and collapse, forming a dense filament of gas that will fragment if the collapse perpendicular to the filament is stopped temporarily, e.g. due to heating by the release of gravitational energy. In this case, the simulations show that the fragments move along the filament and merge.

3. NUMERICAL SIMULATIONS OF COLLIDING BONNOR-EBERT SPHERES

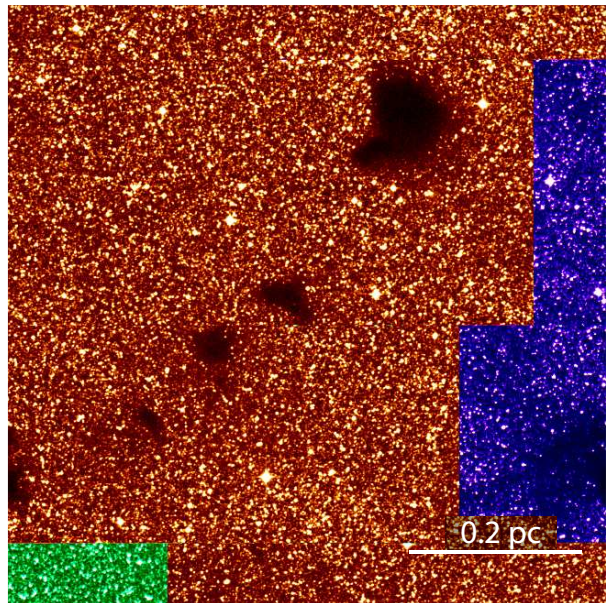
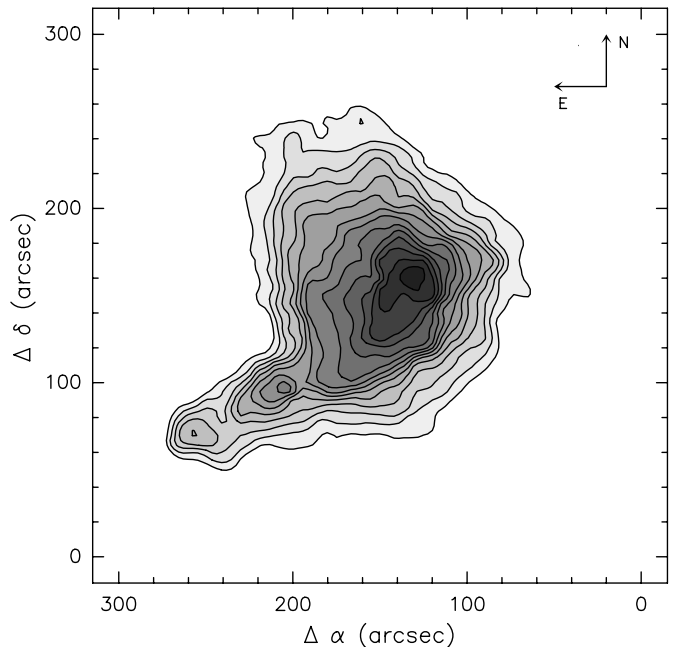


FIG. 1.— The upper panel shows the dust column density map of Barnard 68 (Alves et al. 2001a). About a 1000 measurements of line of sight extinction towards background stars were used to construct this map. Contours start at 2 magnitudes of optical extinction (A_V), and increase in steps of 2 magnitudes. The peak column density through the center of the cloud is about 30 magnitudes of visual extinction. The optical image ($0.68\mu\text{m}$) of Barnard 68 (upper right) and its immediate surroundings to the South-West are shown in the lower panel. These clouds are part of the larger (10 pc) Pipe Nebula complex. Image from the Digitized Sky Survey.

We studied the collision of Barnard 68 with a small core numerically. The isothermal hydrodynamical equations of merging gaseous globules were integrated using the SPH algorithm (Wetzstein et al. 2008) with 40000

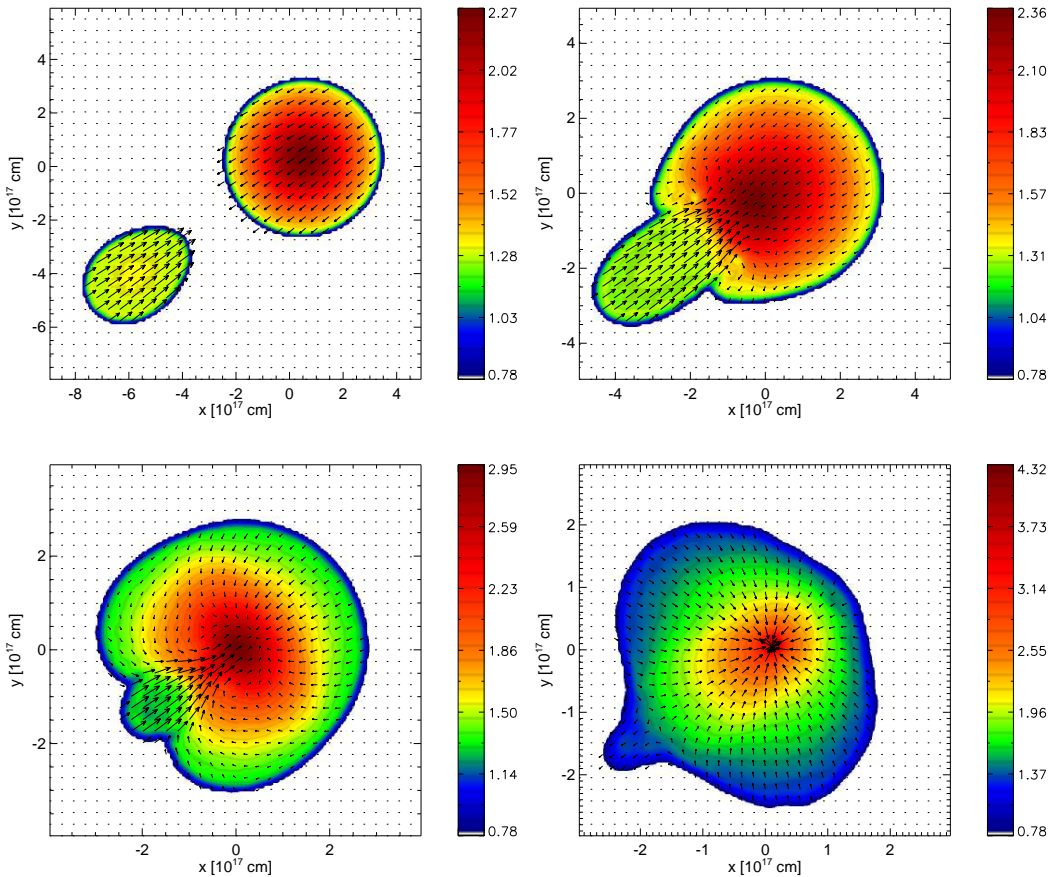


FIG. 2.— Snapshots of our standard model, a merger simulation of a 0.21 solar mass bullet with a 2.1 solar mass main cloud that is characterised initially by a dimensionless parameter $\xi_{max} = 6$. The panels show 2-dimensional cuts through the equatorial plane of the 3-dimensional SPH simulation. Colors indicate the logarithm of the gas density in units of $4 \times 10^{-15} \text{g/cm}^3$. The arrows show the velocity field. The upper left diagram shows an early phase before the collision, 0.9 million years after the start of the simulation. The maximum velocities are 0.16 km/s. The bullet is already tidally elongated. The upper right diagram represents the present state of Barnard 68, 1.7 million years after the start of the simulation. The lower left and lower right panels show the system 1.95 million years and 2.1 million years after the start of the simulations. The maximum velocities are 0.46 km/s and 4 km/s, respectively. As soon as the bullet has merged with the main cloud, the whole system begins to collapse with large infall velocities and the formation of a high-density central core.

SPH particles for the main cloud and 4000 particles for the bullet. The confining effect of the external pressure P_{ext} was taken into account by modifying the equation of state: $P = \rho c_s^2 - P_{ext}$.

Two equilibrium cores with masses of 2.1 and 0.21 solar masses, respectively, were generated, adopting an isothermal sound speed of $c_s = 0.2$ km/s and no initial spin. In order to generate initial conditions for different values of ξ_{max} , we determined the corresponding dimensionless mass m (see Appendix) and from that calculated the required external pressure

$$P_{ext} = m^2 \frac{c_s^8}{G^3 M^2}. \quad (2)$$

To guarantee hydrostatic equilibrium, the cores were allowed to relax in isolation for 20 dynamical timescales. At the end of this phase their surface density profiles followed the expected Bonnor-Ebert solution with high accuracy. We took a main cloud with $\xi_{max} = 6$, corre-

sponding to a dimensionless mass of $m_{B68} = 1.179$ and an external pressure of $P_{ext} = 6.8 \times 10^{-12} \text{dyn cm}^{-2}$. The bullet is embedded in the same pressure environment. Therefore its dimensionless mass is $m_{bull} = 0.1 \times m_{B68} = 0.118$, corresponding to $\xi_{max} = 1.16$. For the standard model the bullet was placed at rest at a distance $d=0.3$ pc from the main cloud. The mutual gravitational force accelerated the bullet towards the main cloud, leading to a collision after 1.7 million years.

Fig. 2 shows the evolution of our standard model. The bullet is accelerated towards the main cloud by their mutual gravitational attraction. After 1.7×10^6 yrs the bullet collides with the main cloud with a relative velocity of 0.37 km/s which is supersonic. As seen in the upper right diagram of Fig. 2, the bullet is now clearly tidally elongated and its momentum is large enough for its gas to penetrate deeply into the main cloud, all the way into its central region. An interesting side effect of this process is that CO-rich gas from the bullet and the outer parts of the main cloud is funneled into the CO-depleted

core region of the main cloud which should increase the core's CO abundance. Theoretical models of detailed molecular line observations indicate depletion of CO in the inner region of Barnard 68 as a result of molecule freeze-out onto grain surfaces (Bergin et al. 2006; Maret et al. 2007). The models predict chemical timescales of only $1\text{--}3 \times 10^5$ yrs to reach the observed degree of CO depletion which is an order of magnitude shorter than the expected lifetime of the gas clump. For ages of order a million years freeze-out should however be more efficient and the $\text{C}^{18}\text{O}(1\text{--}0)$ line intensities should be smaller than measured. The merger might increase the central CO abundance enough in order to solve this problem. Note, that these conclusions are still a matter of debate due to the uncertainties in the chemical network and the treatment of radiation transport as well as due to uncertainties in understanding the formation and past evolution of the globule. The affect of the current merger on the internal chemical structure of Barnard 68 will be studied in details in a subsequent paper.

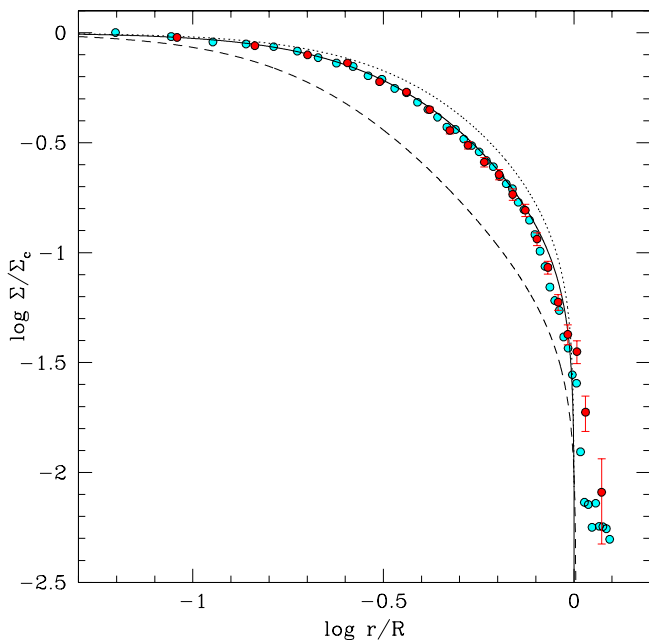


FIG. 3.— The cyan points show the surface density structure $\Sigma(r)$ of the main cloud at the onset of merging with the bullet (see the upper right panel of Fig. 2). Here Σ is normalized to the central value $\Sigma_c \equiv \Sigma(r=0)$. The radius r is normalized to the maximum radius R (the theoretical edge) of the main cloud if it would follow a perfect Bonnor-Ebert profile. Red points with error bars show the observed structure of Barnard 68 as determined from near IR dust extinction measurements. The dotted, solid and dashed lines show theoretical Bonnor-Ebert spheres with $\xi_{max} = 6, 7$ and 10 , respectively. The numerical simulations are in excellent agreement with the observations. The low surface density points beyond the theoretically expected edge, i.e. for $r > R$ correspond to perturbed gas at the edge of the main cloud and gas from the infalling bullet.

The observed bullet, despite having the same mass as in the simulation, is more elongated and less spherical. This is a result of the fact that the bullet itself has experienced a merger recently. In our standard simulation we did not take this into account. We have however verified through test simulations that the physics of the encounter and the subsequent evolution of the system does

not depend sensitively on the adopted initially elongation of the infalling substructure or whether two almost attached substructures, each with 50% the bullet's mass, merge with the main cloud.

The collision disturbs the main cloud, leading to characteristic features that can be compared with observations. Fig. 3 shows that the surface density distribution (cyan points) of the core can still be described very well by a Bonnor-Ebert fit (solid line). However, compared to the initial distribution with $\xi_{max} = 6$ (dotted line), its profile is now characterized by a larger value of $\xi_{max} = 7 \pm 0.2$ (solid line) which is in the unstable regime. The structure of the simulated globule is in excellent agreement with the observations (red points in Fig. 3). Note that there is gas beyond the theoretical Bonnor-Ebert edge R of the main cloud which mainly belongs to the infalling bullet.

Is there evidence for the collision in line-profile measurements of the line-of-sight velocity distribution? Adopting a projection angle of 90 degrees, that is a line-of-sight precisely perpendicular to the orbital plane, our simulations show that for an initially quiescent main cloud without strong intrinsic oscillations, the gravitational interaction with the bullet triggers a characteristic line-of-sight velocity field that shows infall of the outer envelope of the main cloud with a velocity of order 10 m/s while the ram pressure of the merger leads to an outflow of gas from the center with a velocity of up to 5 m/s. Indeed, gas outflow from the center and infall of the outer envelope has been detected (Maret et al. 2007). However the measured velocities are a factor of 4 larger than predicted theoretically. This might indicate that the observed velocity structure is still dominated by the expected natural stable oscillations (Redman et al. 2006; Broderick et al. 2007) of Barnard 68, prior to the encounter. An impact exactly perpendicular to the line-of-sight is however unlikely. We find that the velocity distribution along the line-of-sight depends on the adopted projection angle. For projection angles of 60–80 degrees, the line-of-sight velocity profiles show mean outer infall motions of 40 m/s as they now contain the signature of the fast encounter, in better agreement with the observations.

B68's observed velocity field (Lada et al. 2003) shows an asymmetric distribution with coherent infall with a velocity of 120 m/s in the southeastern part corresponding to the interaction region of the two clumps. If this is interpreted as the line-of-sight velocity part of the bullet and assuming an impact velocity of 0.4 km/s, the inclination angle would be 73 degrees. In general, for projection angles of 60 degrees or larger (probability of 50%) the line-of-sight velocity distribution of the merger simulations is consistent with a combination of intrinsic oscillations of B68 and gas flows generated as a result of the merger.

4. COLLISION-TRIGGERED COLLAPSE OF BARNARD 68

As shown in the two lower panels of Fig. 2, the main cloud collapses as soon as the bullet has completely merged. This is not surprising as the dimensionless mass of the total system $m_{tot} = m_{B68} + m_{bullet} = 1.3$ is larger than the critical Jeans limit $m_{Jeans} = 1.18$ for a stable Bonnor-Ebert sphere (see Appendix). An initial stability parameter of $\xi_{max} = 6$ for B68 however appears rather

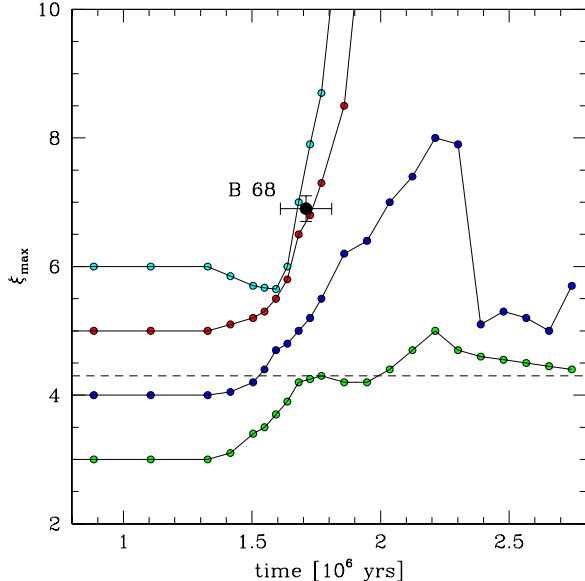


FIG. 4.— Evolution of the dimensionless parameter ξ_{max} of the main cloud, adopting different initial values for $\xi_{max}(t=0)$. The main cloud experiences a collision with a bullet at $t=1.3$ million years. The dashed curve divides the diagram into two regions. For main clouds with $\xi_{max}(t=0) < 4.3$, the dimensionless mass m after the merger is still smaller than the critical mass for gravitational collapse ($m_{crit} < 1.15$). They go through a violent relaxation phase and then settle into a new stable Bonnor-Ebert state. Objects that start initially above this line cannot achieve stability after the merger and therefore collapse. The green and blue points show two stable merger simulations that started with main clouds of $\xi_{max} = 3$ and 4, respectively. The red and cyan points correspond to unstable mergers with initial values of $\xi_{max} = 5$ and 6. The black point with error bars shows the observed evolutionary state of Barnard 68 which is in very good agreement with an unstable merger that leads to gravitational collapse.

fine tuned. What is the range of ξ_{max} values that is in agreement with the observations? And could Barnard 68 survive the encounter as a stable cloud?

Fig. 4 shows the time evolution of the dimensionless parameter ξ_{max} for four simulations with different values of the confining external pressure that correspond to different initial values of ξ_{max} . The mass of the main cloud and the bullet were the same as in the standard model. Theoretically, main clouds with initial values of $\xi_{max} \leq 4.3$ (dashed line), corresponding to the dimensionless mass $m \leq 1.07$ could survive a merger with a bullet of 10% their mass as $m_{tot} < m_{Jeans}$. Indeed we find that for initial values of the main cloud of $\xi_{max} = 5$ or 6 the system collapses. On the other hand, the two simulations with initial values of $\xi_{max} = 3$ or 4 after a phase of compression re-expand and within several dynamical timescales achieve a new equilibrium state that is consistent with their increased total mass. As an example of a stable merger, Fig. 5 shows snapshots for a $\xi_{max} = 3$ main cloud. After a phase of oscillations, the system settles into a new hydrostatic equilibrium state. Note that the clouds in this simulation are larger than in the standard model (Fig. 2) due to the reduced external pressure.

Could Barnard 68 have started with a value lower than $\xi_{max} \leq 4.4$, that is could it survive the collision as a stable, starless core? The observations provide information not only on the density structure, characterized by ξ_{max}

but also on the phase of merging, that is the evolutionary time. The black point in Fig. 4 shows the location of Barnard 68 in the ξ_{max} versus time diagram. The evolutionary time is no free parameter as it is determined by comparing the relative positions of both cores in the simulations with the observations. Excellent agreement exists for initial conditions that correspond to $\xi_{max} \geq 5$ and that lead to gravitational collapse. Interestingly, the situation is different for smaller values. Although the merger simulation with $\xi_{max} = 4$ temporarily leads to a distorted density profile with values of $\xi_{max} = 7$ as observed for Barnard 68, these values are reached in a rather late phase of merging after the bullet has disappeared within the main cloud. We therefore conclude that Barnard 68 is in fact experiencing a fatal merger that leads to gravitational collapse.

5. CONCLUSIONS

We are then in the fortunate situation of witnessing the collapse of a Bok globule and the formation of a star like our Sun, or a low-mass multiple stellar system, in the relative nearby solar neighborhood. Given the distance to this cloud this would make Barnard one of the nearest star forming clouds to Earth, a perfect laboratory to investigate the early phases of gravitational cloud collapse. Barnard 68 has probably been stable for several million years. However its current fatal impact with an object of 10% its mass has made this globule gravitationally unstable which is revealed by a dimensionless structural parameter $\xi_{max} = 6.9 \pm 0.2$ that already exceeds the critical value expected for a stable cloud. The impact is also mixing gas from the chemically less evolved outer parts of the main cloud as well as the CO-rich gas of the bullet with the CO depleted gas in the center of Barnard 68.

Within the next 10^5 years the bullet will be completely engulfed by Barnard 68 which at the same time will develop a centrally peaked surface density profile (dashed curve in Fig. 3) and a velocity field consistent with large-scale gravitational collapse. 10^5 years later a new infrared source will appear in its central region. An isolated star like our Sun will be born in our immediate Galactic neighborhood, probably surrounded by a residual dusty accretion disk where planets might start forming.

We thank Charlie Lada for valuable comments. The numerical simulations were performed on the local SGI-ALTIX 3700 Bx2, which was partly funded by the Cluster of Excellence "Origin and Structure of the Universe

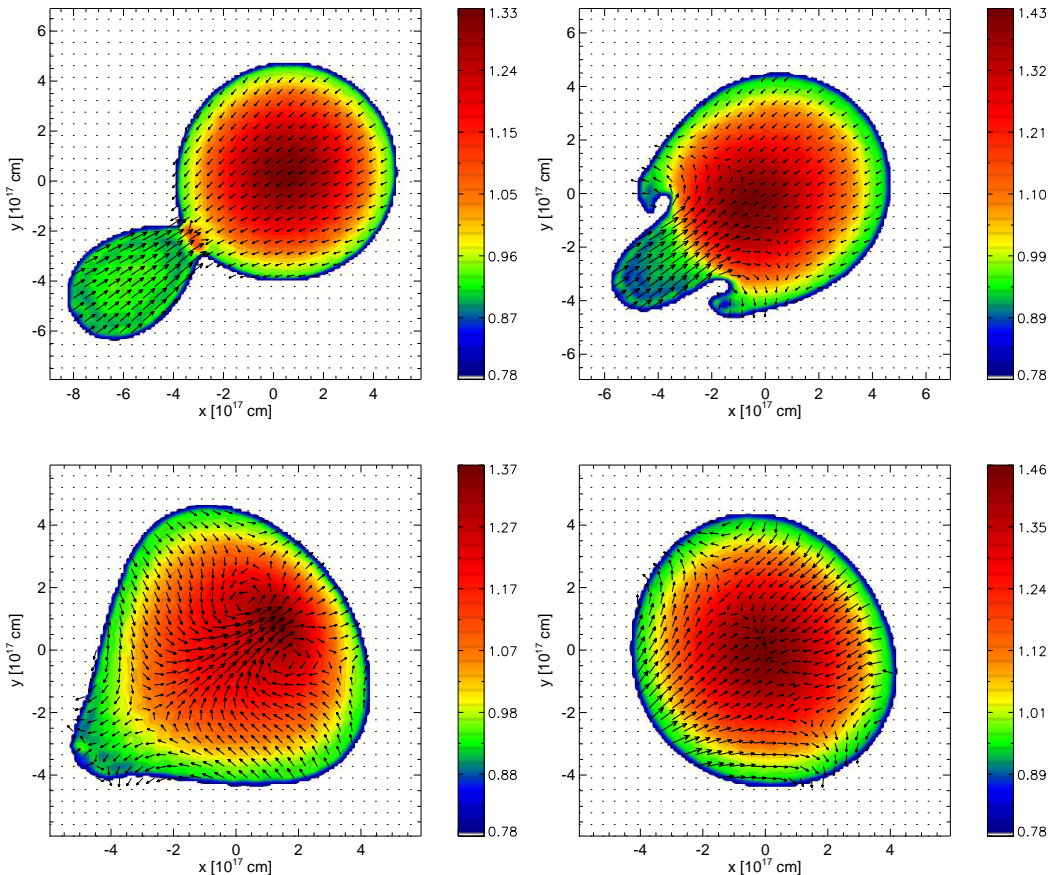


FIG. 5.— Same as Fig. 2, however now with a main cloud that is characterised by $\xi_{max} = 3$. The upper left, upper right, lower left and lower right panels show the state of the system at evolutionary times of 0.9 million years, 1.7 million years, 3.5 million years and 17 million years, respectively. The maximum velocities are 0.16 km/s, 0.25 km/s, 0.017 km/s and 0.013 km/s, respectively. Note that, in contrast to the unstable merger case, here the maximum velocity decreases in the late phases when the system goes through a period of damped oscillations and then settles into a new pressure confined equilibrium state.

APPENDIX

The structure of pressure confined, self-gravitating and isothermal gas spheres in hydrostatic equilibrium is determined by the hydrostatic equation

$$\frac{1}{\rho} \vec{\nabla} P = -\vec{\nabla} \Phi \quad (3)$$

where ρ and P is the gas density and the pressure, respectively. The gravitational potential Φ can be calculated from the density distribution, using the Poisson equation

$$\nabla^2 \Phi = 4\pi G \rho \quad (4)$$

with G the gravitational constant. The pressure is given by the equation of state $P = \rho c_s^2$ where c_s is the constant isothermal sound speed.

In the case of spherical symmetry, these equations can be combined, leading to a differential equation for Φ :

$$\frac{1}{r^2} \frac{d}{dr} \left(r^2 \frac{d\Phi}{dr} \right) = 4\pi G \rho_c \exp \left(-\frac{\Phi(r)}{c_s^2} \right). \quad (5)$$

with

$$\rho(r) = \rho_c \exp \left(-\frac{\Phi(r)}{c_s^2} \right) \quad (6)$$

and $\rho_c = \rho(r=0)$ the central density. We now introduce the dimensionless variables $\Psi \equiv \Phi/c_s^2$ and $\xi \equiv (4\pi G \rho_c / c_s^2)^{0.5} r$. Equation 5 then reduces to a special form of the Lane-Emden equation

$$\frac{1}{\xi^2} \frac{d}{d\xi} \left(\xi^2 \frac{d\Psi}{d\xi} \right) = \exp(-\Psi). \quad (7)$$

Given the inner boundary conditions $\Psi(\xi=0) = 0$ and $\left(\frac{d\Psi}{d\xi} \right)_{\xi=0} = 0$, equation 7 can be integrated numerically.

The left panel of Fig. 6 shows the radial distribution of $\rho/\rho_c = \exp(-\Psi)$ as function of the dimensional radius ξ .

If the gas sphere is confined by an external pressure P_{ext} its edge with radius R is determined by the condition $\rho(R) = \rho_c \exp(-\Psi_{max}) = P_{ext}/c_s^2$, that is

$$R = \left(\frac{c_s^2}{4\pi G \rho_c} \right)^{1/2} \xi_{max} \quad (8)$$

with $\Psi(\xi_{max}) = \Psi_{max} = -\ln \left(\frac{P_{ext}}{\rho_c c_s^2} \right)$.

The total mass of the system is

$$M(r) = 4\pi \int_0^R r'^2 \rho(r') dr' = \quad (9)$$

$$4\pi \rho_c^{-1/2} \left(\frac{c_s^2}{4\pi G} \right)^{3/2} \left(\xi^2 \frac{d\Psi}{d\xi} \right)_{\xi=\xi_{max}}$$

We now can define the dimensionless mass

$$m \equiv \frac{P_{ext}^{1/2} G^{3/2} M}{c_s^4} = \left(4\pi \frac{\rho_c}{\rho(R)} \right)^{-1/2} \left(\xi^2 \frac{d\Psi}{d\xi} \right)_{\xi=\xi_{max}} \quad (10)$$

The right panel of Fig. 6 shows $m(\xi_{max})$. m reaches a maximum $m_{max} = 1.18$ for $\xi_{max} = 6.5$, corresponding to a density contrast of $\rho_c/\rho(R) = 14$. No equilibrium

solution exists for larger masses. A stability analysis also shows that for $\xi_{max} > 6.5$ a gaseous configuration is unstable

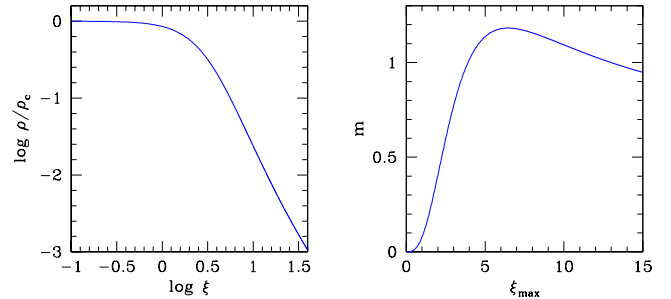


FIG. 6.— The left panel shows the density distribution, normalized to the central density ρ_c of an isothermal, self-gravitating gas sphere as function of its dimensionless radius ξ . The dimensionless mass m of a Bonnor-Ebert sphere with radius ξ_{max} is shown in the right panel.

REFERENCES

- Alves, J., Lada, C. & Lada, E. 2001a, *The Messenger*, 103, 1
 Alves, J., Lombardi, M., & Lada, C.J. 2007, *A&A*, 462, L17
 Alves, J., Lada, C.J. & Lada, E.A. 2001b, *Nature*, 409, 159
 Bergin, E.A., Maret, S., van der Tak, F.F.S., Alves, J., Carmony, S.M. & Lada, C.J. 2006, *ApJ*, 645, 369
 Bok, B.J., 1948, in *Centennial Symposia*, 53
 Bok, B.J., & Reilly, E.F. 1947, *ApJ*, 105, 255
 Bonnor, W.B. 1956, *MNRAS*, 116, 351
 Broderick, A.E., Keto, E., Lada, C.J. & Narayan, R. 2007, *ApJ*, 671, 1832
 Broderick, A.E., Narayan, R., Keto, E. & Lada, C.J. 2008, *ApJ*, astro-ph/0804.1790
 Burkert, A. & Bodenheimer, P. 1993, *MNRAS*, 264, 798
 Burkert, A. & Bodenheimer, P. 1996, *MNRAS*, 280, 1190
 Burkert, A. & Hartmann, L. 2004, *ApJ*, 616, 288
 Lada, C.J., Bergin, E.A., Alves, J.F. & Huard, T.L. 2003, *ApJ*, 586, 286
 Lada, C.J., Muench, A.A., Rathborne, J., Alves, J.F. & Lombardi, M. 2008, *ApJ*, 672, 410
 Lombardi, M., Alves, J. & Lada, C.J. 2006, *A&A*, 454, 781
 Maret, S., Bergin, E.A. & Lada, C.J. 2007, *ApJ*, 670, L25
 Redman, M.P., Keto, E. & Rawlings, J.M.C. 2006, *MNRAS*, 370, L1
 Truelove, J.K., Klein, R.I., McKee, C.F., Holliman, II, J.G., Howell, L.H., Greenough, J.A. & Woods, D.T. 1998, *ApJ*, 495, 821
 Wetzstein, M., Nelson, A.F., Naab, T. & Burkert, A. 2008, *astro-ph/0802.4253*